THE JOURNAL OF PHYSICAL CHEMISTRY C

Article

A Fresh Molecular Look at Calcite-Brine Nanoconfined Interfaces

Alexsandro Kirch, Sylvia Mueni Mutisya, Veronica M. Sanchez, James Moraes de Almeida, and Caetano Rodrigues Miranda

J. Phys. Chem. C, **Just Accepted Manuscript** • DOI: 10.1021/acs.jpcc.7b12582 • Publication Date (Web): 26 Feb 2018

A Fresh Molecular Look at Calcite-Brine Nanoconfined Interfaces

Alexsandro Kirch,[†] Sylvia M. Mutisya,[‡] Verónica M. Sánchez,[¶] James M. de Almeida,[†] and Caetano R. Miranda[*,†]

[†]*Instituto de Física, Universidade de São Paulo, CP 66318, 05315-970, São Paulo, São Paulo, Brazil*

[‡]*Nanociências e Materiais Avançados, Universidade Federal do ABC, Santo André, São Paulo, Brazil*

[¶]*CSC, CONICET, Godoy Cruz 2390, 1425, Buenos Aires, Argentina*

E-mail: cmiranda@if.usp.br

Abstract

Calcite-fluid interface plays a central role in geochemical, synthetic and biological crystal growth. The ionic nature of calcite surface can modify the fluid-solid interaction, the fluid properties under spatial confinement and can also influence the adsorption of chemical species. We investigate the structure of solvent and ions (Na, Cl and Ca), at calcite-aqueous solution interface under confinement, and how such environment modify the water properties. To properly investigate the system, molecular dynamics simulations were employed to analyze the hydrogen bond network and to calculate NMR relaxation times. Here, we provide a new insight with additional atomistically detailed analysis by relating the topology of the hydrogen bond network with the dynamical properties in nanoconfinement interfaces. We have shown that the strong geometrical constrains and the presence of ions, do influence the hydrogen bond network, resulting

in more extended geodesic paths. Hydrogen bond branches connect low to high dynamics molecules across the pore and hence may explain the glue-like mechanical properties observed in confinement environment. Moreover, we showed that the surface water observed at calcite interface is characterized by slow transversal spin relaxation time (T_2) and highly coordinated water molecules. The physical and electrostatic barrier emerged from the epitaxial ordering of water result in a particular ionic distribution which can prevent the direct adsorption of a variety of chemical species. The implications of our results delineate important contributions to the current understanding of crystallization and biomineralization processes.

Introduction

Phase transition anomalies[1] and formation of ice-like structures[2] are some examples of a variety of phenomena which can emerge in nanoscopic environments with water at or near a solid interface. Investigating water properties under such conditions is essential to understand the underlying porous media mechanisms in geochemical, synthetic and biological crystal growth[3]. Such processes often occur with water at some salt concentration, and currently, the structure of solvent and ions at solid-solution interfaces, as well as, the effect of ions on water properties under confinement and its implications on the processes involved in this kind of systems are poorly understood[4].

Previous studies explored the effect of spatial confinement on the hydrogen bond network and the dynamics based solely on pure water[5–8]. According to Dore[7], water in a confined geometry shows significant modification on its hydrogen bond structure in comparison to the bulk phase. The author showed by neutron diffraction spectroscopy, the formation of an extended hydrogen bonded network similar to that observed in amorphous ice. Different experimental techniques revealed that the water viscosity increases and the diffusion coefficient decreases[9,10]. The slowdown of water dynamics confined by narrow hydrophilic walls is a common feature in these systems.

On the other hand, the role of salt ions on water structure and dynamics has been widely explored[11–14]. Both experimental and theoretical studies describe the effect of ions on the hydrogen bond network in terms of making and breaking capability[12], i.e, certain type of ions break and others make hydrogen bonds. The effects of ions on the hydrogen bond network translate to changes in water viscosity according to these works. Furthermore, some studies indicate that electrolyte aqueous solutions have similar effect as pressure on the water hydrogen bond network[14].

Few authors have drawn together some aspects of the complexity found in a system which involve the effects of ions, solid surface interface and nanoconfinement on water properties[15–21], but many knowledge gaps still remain. Currently, it is difficult to separate these individual contributions by experimental techniques. The progress achieved so far in this research field can be expanded or complemented by computational simulation through an atomistic perspective, contributing to a predictive understanding of some important aspects involved in crystallization process.

In this article, we report the results of a systematic study performed with the aim of bringing a new insight about the effect of ions on the structure and dynamics of water under spatial confinement retained by calcite ($CaCO_3$) pores. The complexity found in the system required the adoption of an original approach carried out to properly understand these important aspects arising in the porous media. It was achieved by combining molecular dynamics simulations with hydrogen bond network analysis based on graph theory and Nuclear Magnetic Resonance (NMR) modeling. We were able to properly isolate the contributions of the ions, surface and confinement on the network structure of hydrogen bonds and to relate it with the dynamical properties accessed by the transverse spin relaxation time analysis. Measurements of the ^1H transverse relaxation times (T_2) enable definite assignment of water protons of different mobilities to the observed diffusion processes and, hence, can be used to identify structural changes in porous minerals. Furthermore, the water branch aspect seen from a new perspective based on graph geodesic analysis revealed the formation of more ex-

tended hydrogen bond geodesic paths under extreme confinement and salt ions. Substantial amount of water branches formed by continuous hydrogen bonds cross the pore and connect low to high dynamics molecules under extreme confinement. The response on water dynamics was observed on the transverse spin relaxation indicating an overall slowdown diffusion. We also highlight the observation of an electrostatic and physical barrier near the calcite surface due to the epitaxial water. The ice-like resembling structure is characterized by slow T_2 and with prevalence of highly coordinated water molecules. The spatially alternated electrostatic potential resulting from high ordering of water dictates the ionic distribution inside the pores, thus reducing the probability of desolvating and attaching of foreign chemical species. This may have significant implications and can contribute to the current understanding of the crystallization and biomineralization processes. We discuss the physical indications and potential significance of our results on crystal growth and dissolution processes.

Methods

Molecular dynamics

The classical molecular dynamics simulations were performed using the large atomic massively parallel simulator (LAMMPS)[22] package. The calculations were performed in the NPT ensemble with an anisotropic barostat for the thermodynamic equilibration at 300 K and 1 atm, following by a NVT production run for 5 ns with a time step of 0.5 fs. Temperature and pressure were controlled based on the Nosé-Hoover methods[23,24]. In addition, the non-bonded pair interactions are truncated at a cutoff distance of 9 Å and the long-range electrostatic interactions were solved by the PPPM[25] method. The number of ions and water molecules inside each investigated pore were specified in Table S1.

To describe the inter atomic interactions, we used the force field developed by Raiteri et al.[26,27] for a calcite–water interface. This force field allows for flexibility of the carbonate ion and the water molecules are described by the SPC-Fw model[28]. To account for the interac-

tions of sodium and chlorine ions in API–brine, we employed parameters from Grossman et al.[29] work. The Ca–O_w parameter obtained by Raiteri and co–workers[26,27] is used here to describe its interaction with water.

NMR modeling

The self-diffusion coefficient D — a measure of the rate of displacement of water molecules from their equilibrium position — was calculated from the mean square displacement Einstein relation[30];

$$D = \lim_{t\to\infty} \frac{\langle |\mathbf{r}(t) - \mathbf{r}(0)|^2 \rangle}{6t} \tag{1}$$

where $\mathbf{r}(t)$ is the position vector of the water molecule center of mass at time t. The angular brackets denote an average over time origins and all water molecules. Within the layers, parallel self-diffusion coefficient $D_{||}$ in each layer is given by:

$$D_{||}(\{z\}) = \lim_{t\to\infty} \frac{\langle \Delta\mathbf{r}(t)^2 \rangle_{\{z\}}}{4P(t)t} \tag{2}$$

where $\{z\}$ represents the set of molecules that remain in the slab centered at a distance z from the surfaces during the interval $[0, t']$. $P(t)$ is the survival probability function ($P(t) = 1/T \sum_{t=1}^{T} N(t)/N(0)$) which relates the number of molecules $N(t)$ which remain in the slab in the time interval $[0, t']$ to the number of molecules $N(0)$ which were present at the initial time $t = 0$. T is the total number of time steps averaged over.

For the rotational dynamics, we investigate the HH intramolecular vector reorientation which is probed by proton NMR in H_2O experiments[31]. The rotational correlation time τ_c was obtained by fitting the autocorrelation function $C_{HH}(t)$ (second order Legendre polynomial) to a a stretched exponential function $a_0 e^{-(t/\tau_c)^\beta}$ for the confined water and a simple exponential function $a_0 e^{-(t/\tau_c)}$ for the bulk system.

The theoretical calculation of the transverse (T_2) spin relaxation is based on a semiclas-

sical theory developed by Bloembergen, Purcell and Pound (BPP)[32]. According to BPP theory, the transverse NMR relaxation rate of a system involving relaxation of the same nuclear species is given as:

$$\frac{1}{T_2} = \frac{3}{8}\left(\frac{\mu_0}{4\pi}\right)^2 \gamma^4 \hbar^2 I(I+1)[J(0) + 10J(\omega) + J(2\omega)] \tag{3}$$

where, γ, $\hbar$ and I are the gyromagnetic ratio, Planck's constant and spin of the diffusing spins, respectively. μ_0 is the permeability of free space and ω is the Larmor frequency in the applied static field. The spectral density function $J(\omega)$ is obtained from Fourier transform of the correlation function $G(t)$:

$$G(t) \quad = \left\langle \frac{P_2(\cos\phi)}{r_0^3 r^3} \right\rangle \tag{4}$$

where, ϕ is the angle between the water molecule HH vectors $\mathbf{r_0}$ and $\mathbf{r}$ at the initial and later time, respectively. $P_2(cos\phi) = \frac{1}{2}(3\cos^2\phi - 1)$ is a Legendre polynomial averaged over the number of spins and time origins. The pore radius dependence of the T_2 spin relaxation is calculated based on the fast-exchange model[33,34]. In this model, the fluid confined in a pore has two distinct phases: a bulk phase, which has the same relaxation properties as the bulk liquid and a surface phase whose relaxation rate is greatly affected.

Results

Our calcite pore model is based on the crystalline structure with rhombohedral morphology obtained from the crystallographic data published by Markgraph and Reeder[35]. This structure was cleaved to expose the $[10\bar{1}4]$ surface, due to its major stability[36–38]. The slit geometry is the simplest representation of a pore and it allows to investigate spatial confinement effects by progressively varying the surface-surface distance (see Figure S1a). We considered pore sizes ranging from 6 to 1 nm to systematically investigate the confinement ef-

fects emerging in brine within nanoscopic environments. We adopt the American Petroleum Institute (API) brine model which is constituted by 8 wt% of NaCl and 2 wt% of $CaCl_2$.

Brine structure within calcite slit pores

PACKMOL[39] package was used to add water molecules randomly within the slit pores at a density of 1 g/cm^3. Ions were then inserted by randomly substituting water molecules. In addition, ions were only included in the pore center, preserving each hydration shell, thus avoiding their spurious presence near the surfaces trapped in local minima[40]. After the system reached thermodynamic equilibrium under fully atomistic molecular dynamics simulations, it was observed that water molecules are structured in layers near the solid surface interface, similar to the ones observed in pure water system[5,21,41] (see Figures 1a–d). Under ambient conditions, an adsorbed region is always present at hydrophilic surfaces and it is attributed to the strong interaction between water and calcite. According to our previous work[5] and in agreement with experimental results[42], the water density profile exhibits three distinguishable peaks, approximating bulk values beyond 8.0 Å from the calcite surface. Water molecules belonging to layers 1 and 2 (Figures 1a–d) interact directly with the calcite surface[5], and therefore, they constitute the surface or adsorption layer. Inside layer 3 are water molecules disconnected with calcite surface, but their density is affected by the ordering of surface layer and the ionic steric effect. Calcite systems with slit pore sizes ranging from 6 to 2 nm display similar density profiles as shown in Figure 1a. However, the system with 1 nm pore size (Figure 1c) has an overlap of right and left side density profiles due to extreme confinement, resulting in differences — with respect to the other investigated systems — only in the density of layer 3 and the pore center, thus leaving layers 1 and 2 unaltered. Our layered analysis following this work is based on the water structuring observed in the density profile. Additional layers (layers 4, 5 and 6), separated by 5.0 Å as depicted in Figures 1a and 1b, were considered to investigate systematically the effect of confinement.

Besides the water molecule positions, the calcite hydrophilicity also determine the water

dipole moment orientation with respect to the surface normal vector (see Figures 1b and 1d). This is observed mainly on water molecules belonging to the surface layer, since they interact directly with calcite surface. Some water molecules are linked to a surface calcium via their oxygen atoms, while other ones form a hydrogen bond with the calcite surface oxygen atoms, resulting in preferential orientation angles[43]. All investigated systems show similar dipole moment distributions for the surface layer. The ordering of water molecules revealed by dipole moment orientation analysis starts disappearing inside layer 3 and reach bulk-like behavior beyond 8.0 Å from the calcite surface. These results are similar to the ones observed in pure water under the same conditions[5], showing that the investigated ions preserve the layered aspect of the water density profile and the dipole moment angle distribution.

Layered distribution appear also in the Cl^- and Na^+ density profiles (Figure 1a), but according to our observation, the mechanism which explain this behavior is different from the one used to describe the epitaxial ordering of water. Although our pore model is charge neutral, the calcite surface show strong local variation of charge due to the alternate arrangements between their ionic groups[21]. Water ordering in well defined layers and orientations creates an alternation of positive and negative excess charge[21,41] (see Figure 2a), leading to an electrostatic potential profile as shown in Figure 1b (white line). Consequently, the ions are not structured by layers directly due to the ionic nature of the surface, as one could intuitively expect, but due to the electrostatic potential arising from water structuring. In practice, the positions of the regions with larger charge density exhibited by Na^+ (Cl^-) ions (see Figures 2b and 2c) do not correspond to the negative (positive) charge exhibited by the $CO_3^{2-}(Ca^{2+})$ group on calcite surface along the y axis, but it is associated with the accumulation region of negative (positive) charge observed on the two-dimensional density distribution of the water charge (Figure 2a). Therefore, the Na^+ and Cl^- distribution is influenced by this potential, while Ca^{2+} ions are located more at the pore center due their larger hydration shell[21] (see Figure 2d). Furthermore, the systems with 6 to 2 nm pore sizes

exhibits ionic density profiles which reach more uniform distribution beyond 8 Å from the surface, but the values differ from bulk densities, due to the rearrangements of the ions excluded from surface layer. The system with 1 nm pore size show the largest difference in the ionic concentration with respect to the bulk system in the pore center due to extreme confinement. Nevertheless, the ions do not reach the calcite surface, since substantial energetic penalty has to be overcome, as reported experimentally [21].

Hydrogen bond network analysis

Liquid water exhibit a multiform structure designed by hydrogen bonds with molecules at different degree (number of hydrogen bonds per molecule) of connections forming a complex network [44]. The purpose of the hydrogen bond network analysis was the quantitative elucidation of the effect of the environment (ions, confinements and solid surface interface) on this structure. To address this kind of problem, we adopt the approach based on graph theory implemented in ChemNetworks code [44]. Hydrogen bonds were analyzed based on a set of representative instantaneous atomic configurations taken from molecular dynamics simulations. We considered a geometric criterion for the hydrogen bonds, where the $O - H \cdots O$ angle is greater than 150° and the $O \cdots H$ distance is lower than 2.5 Å [44].

Hydrogen bonds formed between water molecules belonging to the surface layer are ruptured due to the discontinuity on water system at the interface with the calcite surface. However, many of the hydrogen bonds are reformed due to the interaction with the oxygen atoms from carbonate group [5]. The network structure of hydrogen bonds on the adsorption region (see Figures 3a and 3b) are almost unaffected by the ions from API brine. It occurs because they are located far away from the surface (beyond 3.0 Å), consequently, the degree (number of hydrogen bonds) distribution of water molecules inside layer 1 is similar to the one observed in pure water under the same environment. Furthermore, the slight difference observed in the degree distribution of brine with respect to pure water system, both placed in layer 2, is attributed to the few ions which penetrate this layer and the proximity with layer

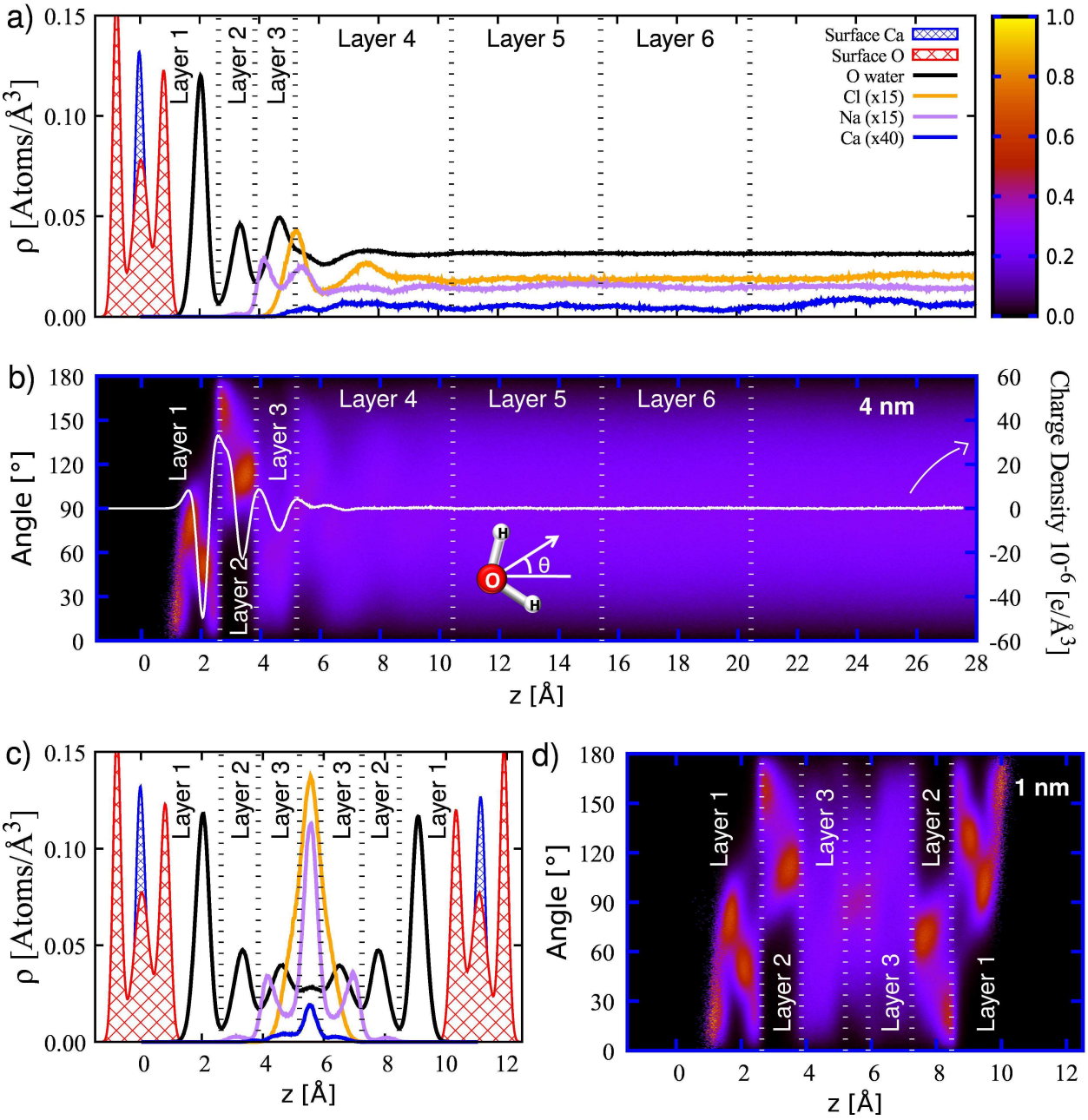

Figure 1: a) Particle density profiles displayed along the 4 nm pore size by the water oxygen; Na, Ca and Cl in the electrolyte aqueous solution ions; and surface Ca and O calcite atoms. or clarity, the atomic density profiles of Na, Cl and Ca are multiplied by a factor of 15, 15 and 40 respectively. The surface limits were defined based on the average positions of surface calcium atoms. Dashed lines delimit the layers. b) Normalized probability distribution of dipole moment orientations with respect the surface normal vector. The electrostatic potential (white line) emerged due to water structuring. This results are representative of the systems from 6 to 2 nm pore sizes. c) Particle density profiles and d) normalized probability distribution of water dipole moment orientations for the 1 nm pore size system.

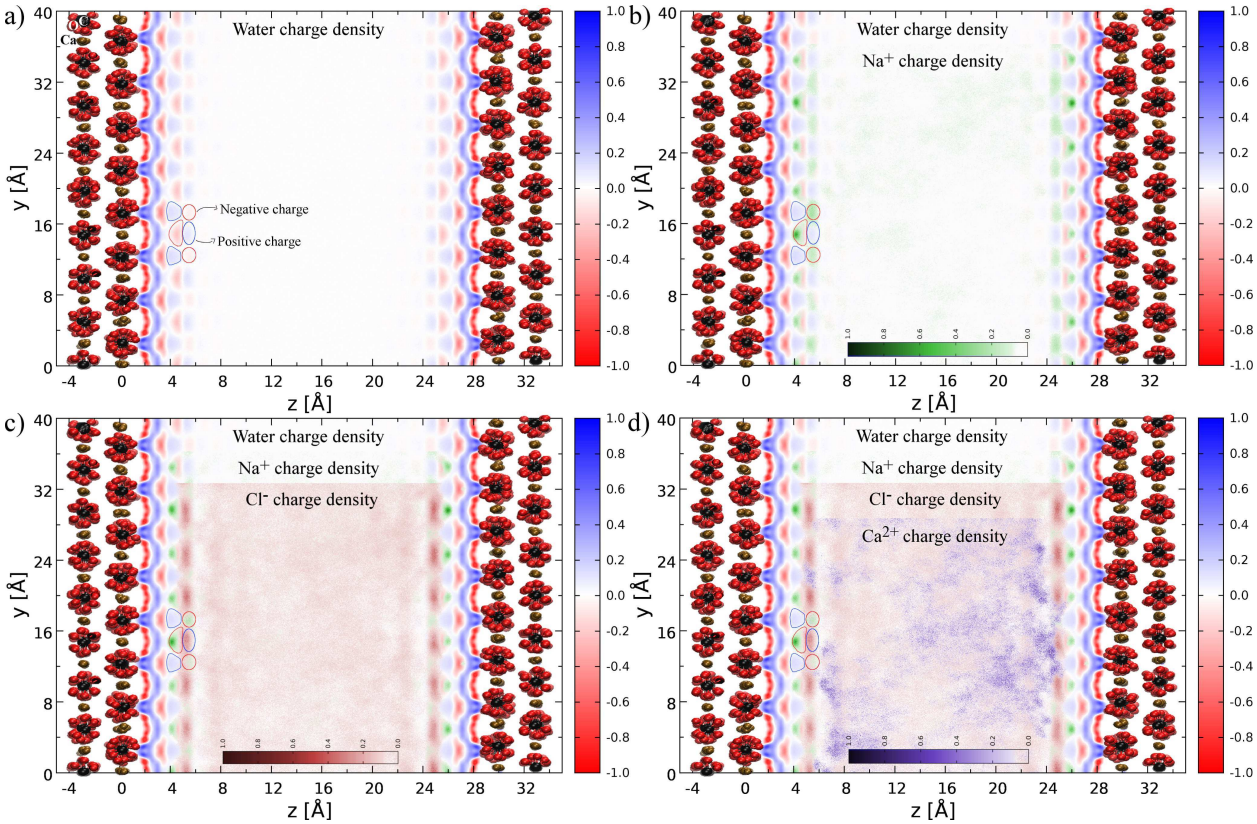

Figure 2: a) Normalized charge density for water inside the 3 nm pore taken over the whole molecular dynamics simulation. Calcite cleaved at $[10\bar{1}4]$ direction, exhibit CO_3^{2-} and Ca^{2+} groups placed alternatively along the y direction. The blue and red colors represent excess of positive and negative charges, respectively. b) Na^+ (green hue), c) Cl^- (red hue) and d) Ca^{2+} (blue hue) normalized charge densities distributions were progressively added. Ions are accommodated in the charge accumulation regions displayed by water ordering.

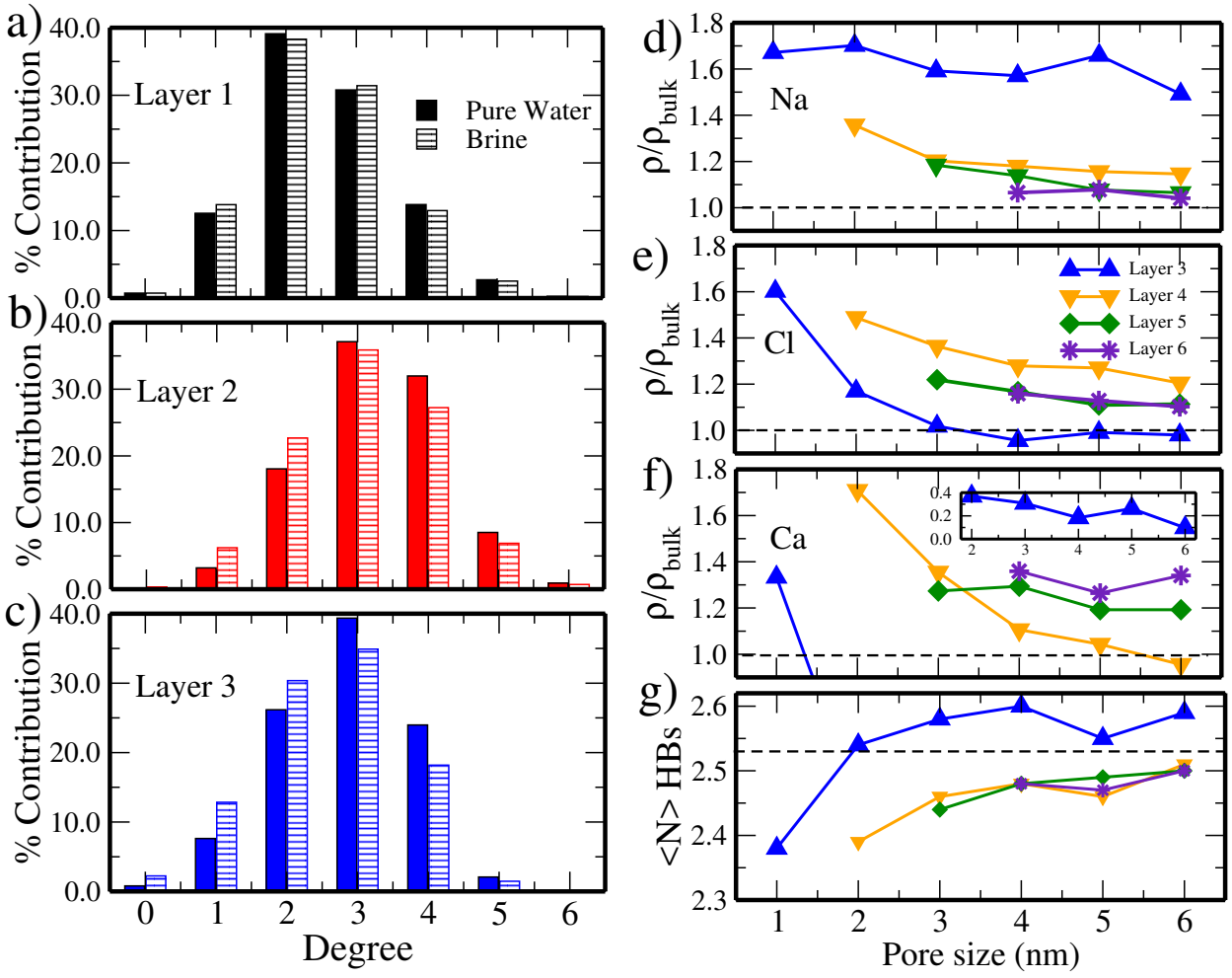

Figure 3: Degree distribution comparison between pure water and brine located inside a) layer 1, b) layer 2 and c) layer 3. Relative particle density — with respect to the bulk values — of d) Na^{+}, e) Cl^{-} and f) Ca^{2+} ions inside each layer for all investigated systems. g) Layered distribution of average number of hydrogen bonds. Standard errors are too small to be represented in this graphic scale.

3 (see Figure 3c): the steric effect which occurs in layer 3 reduce the number of available water molecules to form hydrogen bonds with the molecules located in layer 2. However, the degree distribution of layer 2 remains with a high contribution of four coordinated water molecules which resembles ice-like phases.

The network structure of hydrogen bonds — in the sense of the average number of hydrogen bonds — in subsequent layers is related to the relative Cl^- and Na^+ concentrations, and corroborates with the interpretation retained by many studies[12] about the capability of the ions to make and break hydrogen bonds (see Figures 3d-g). Such response is observed more clearly on layer 3 which exhibits a remarkable unbalanced concentration of these two kind of ions. We demonstrate in a previous work[5] that pure water inside layer 3 (and in subsequent layers) has similar degree distribution as observed in bulk phase, because the molecules located in this region are disconnected from the hydrophilic surface and this result is insensitive with respect to the pore size. However, according to Figure 3g, the average number of hydrogen bonds observed in layer 3 is slightly different from the one observed on brine system at bulk phase. The result matches with the unbalance between Na^+ (making) compared to Cl^- (breaking) concentration in this layer (see Figures 3d and 3e). In practice, the decrease of Cl^- with respect to the Na^+ concentration results in gain in the number of hydrogen bonds. Furthermore, the reduction of the average number of hydrogen bonds observed in layers 4–6 is consistent with the relative increase in Cl^- with respect to the Na^+ concentration. The Ca^{2+} ions have also structure making capability[12] (see Figure 3f), but due to their low density (one order of magnitude lower than Cl^-), their presence preserve the average number of hydrogen bonds.

An assembly of water molecules connected by hydrogen bonds design a network with numerous branches and multiple extensions[44]. Currently, such structure can be accessed by analyzing the graph geodesic through Floyd-Warshall algorithm[44]. In the context of the hydrogen bond network, the graph geodesic is the shortest continuous path designed by a series of hydrogen bonds formed between two water molecules. Their analysis provide

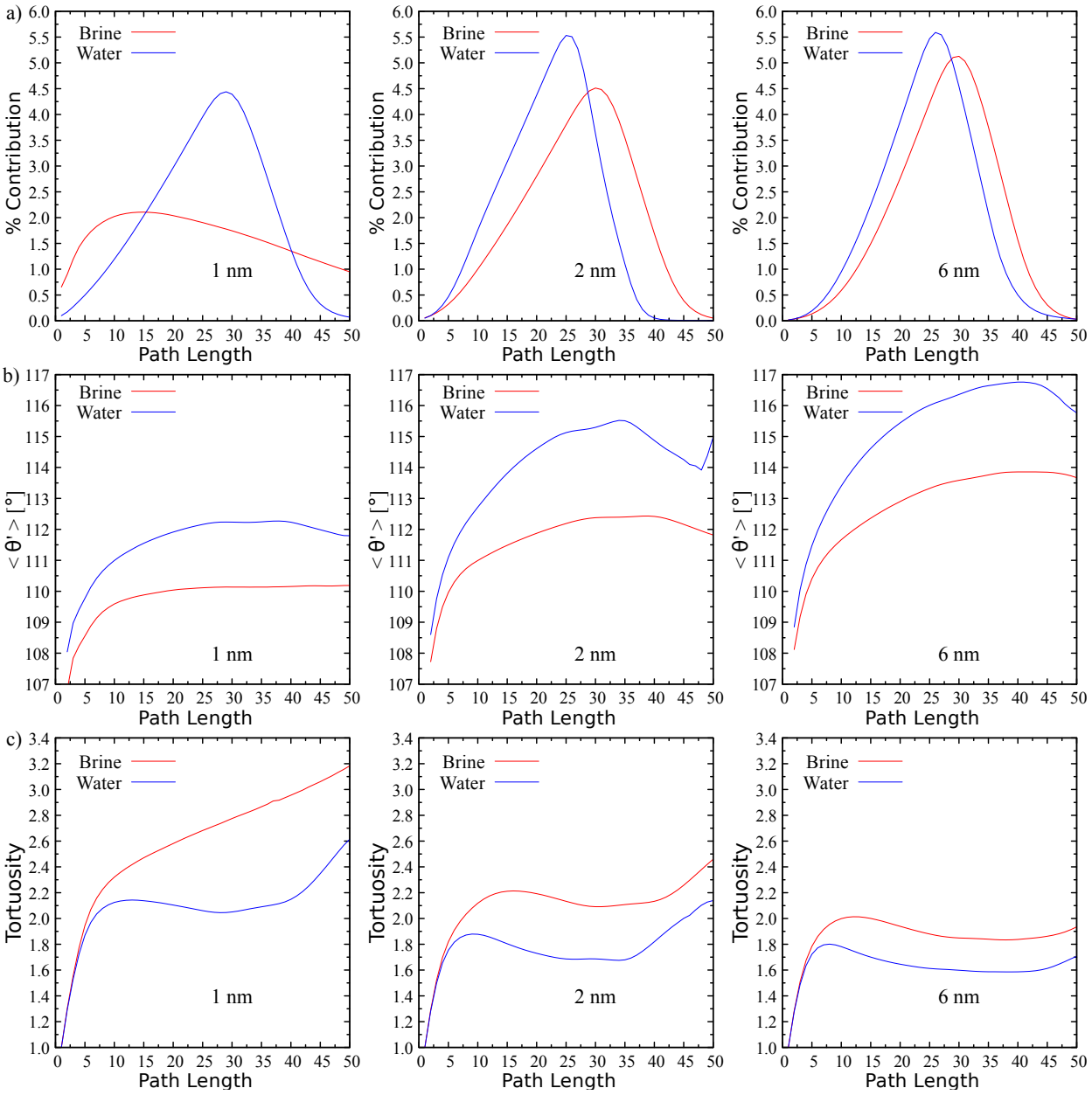

Figure 4: a) Evolution of geodesic path length distributions for brine and pure water confined inside pores sizes with 1,2 and 6nm. Comparison between pure water and brine b) average angle and c) average turtuosity calculated over each path length (see Figure S1 b). The results for the missing pores are shown in Figures S2 a-c). Standard errors are too small to be represented in this graphic scale.

information about the interconnectivity of water molecules and it enables a non–local view over the network topology of the spatially confined brine. In all analyzed pores, we observed an increase — in comparison to the pure water system — in the geodesic path length (see Figure S1b) with the addition of salt ions, as shown in Figure 4a (additional results are shown in the Supplementary Information, Figures S2–7). This effect is enhanced under extreme confinement displayed by systems ranging from 2 to 1 nm pore sizes. In such environment, high percent of geodesic paths cross the pore in the confinement direction and connect high to low dynamics molecules (see Figure S6). A layered analysis through the different regions depicted on Figure 1a was performed to evaluate the origin of this geodesic paths characteristic. We observed the absence of ions on the surface layer results in similar geodesic paths properties for brine and pure water (see Figure S3). Differences between water and brine appear on the path length distributions of layers 4, 5 and 6. However, the property is unrelated to the pore size or layer label (see Figures S4a and S4b). Taken together, these results indicate that larger geodesic paths are displayed to connect two spatially separated water molecules to overcome or contour the network discontinuity imposed by the salt ions and also by the calcite surface on the surface water, this effect being more pronounced in small pores due to the higher surface to volume ratio.

Distortions generated on the hydrogen bond network are also observed through the analysis of the O-O-O triplet angle distribution (see Figure S5). It is characterized by an intense and broad peak corresponding to the tetrahedral coordination of pure water [45]. The salty ions and confinement interface decrease the position of this peak in the angle axis. To explore this effect in more detail, we determined the average angle of the distribution calculated over the water molecules belonging to a specific geodesic path length. The average angle displayed in API brine reach 3° smaller than obtained for the pure water system (see Figure 4b). As a consequence, the geodesic paths are more folded as revealed by the tortuosity analysis shown in Figure 4c. The collective geometric distortion leads to approximately 0.25 Kcal/mol gain (more negative) in potential energy per water molecule (see Figure S7). The

main contributions in the potential energy comes from modifications in the triplet angle distribution, since the hydrogen bond average distance remain the same and the slight differences observed on the average hydrogen bond angle keep the energy invariable. This role is also pore size dependent — as observed mainly in systems with high surface to volume ratio — due to the contribution of surface water which display average triplet angles around 8° lower with respect the remaining system. Such response represent approximately 0.4 Kcal/mol gain in the potential energy per water molecule (see Figure S7). Taken together, the distortions generated on hydrogen bond network revealed by the geodesic path and O-O-O triplet angle analysis can explain the glue-like mechanical properties displayed under extreme confinement [46,47].

Dynamical properties

The hydrogen bond network discussed in the previous section evolves constantly due to continuous dissociation and formation on timescales ranging from tens of femtoseconds to picoseconds [48,49]. In the subsequent sections, we extend the analysis of nanoconfined API brine based on the water dynamics (translational and rotational) which arise as a consequence from this particular hydrogen bond network and how this influences the transverse relaxation time here accessed by NMR modeling.

Diffusion

The diffusivity of the water molecules within the calcite pores was analyzed by plotting the MSD as a function of time (see Figure S8). From these, the normal diffusive linear dependence in time was observed starting from 30 ps and 200 ps for 2-6 nm and 1 nm pores respectively. The calculated reference of self-diffusion coefficient (D) obtained by Equation 1 for water molecules in bulk API brine is $1.98\pm\ 0.01\times10^{-5}$ cm^2s^{-1}, which is lower than the value obtained for bulk water (2.35×10^{-5} cm^2s^{-1}) [5] using the same force field. The D value for water molecules in the API brine under confinement is significantly reduced and it ranges

from 0.23×10^{-5} to 1.46×10^{-5} cm^2s^{-1} from 1 to 6 nm calcite pores (Figure 5a). This trend indeed confirms that the water self-diffusion coefficient is strongly correlated to the pore surface to volume ratio,[50] *i.e*, the smaller the ratio the faster the water mobility. In addition, in confined systems, the translational diffusion of water is highly dependent on the local density and ordering[5]. For the confined API brine, we have shown in the previous section that the inclusion of ions enhances local and non-local ordering, highlighted here by the distortions on the hydrogen bond network (Figures 4a–c). Since the diffusional motion is non-local,[51] our findings shed light on the origin of the overall slowdown of translational displacement in confined aqueous solutions observed experimentally[7].

To disentangle the influence of the surface and ions on water diffusion, we calculated the parallel self-diffusion coefficient $D_{||}$ (Equation 2) of the water molecules which remain in layers 1 to 6 (see Figure 1a) during a certain time interval t'. According to Figure 5b, the diffusion of water is slowest in layers 1 and 2 and very similar to the confined pure water[5]. Due to the absence of ions in these two layers, the slowdown is attributed to the strong water–surface interactions which induce local ordering (see Figures 1b and 1d). Even though experiments have demonstrated that the self–diffusion of water around ions is dependent on structure making/breaking properties[51,52], we obtain an overall downward shift of $D_{||}$ values in layers 4–6, which are in otherwise bulk–like region and dominated by Cl^- structure breaking ions. These findings indicate that the hydrogen bond network distortions revealed in Figures 4a–c) governs the self–diffusion behavior of water in confinement.

Although the surface dominates in slowing down the self–diffusion coefficient $D_{||}$ in 6–2 nm pore size, the trend changes for a 1 nm pore; the parallel diffusion coefficient in all the three layers is comparable. We link this ambiguous diffusion behavior to the high accumulation of the ions at the pore center (see Figure 1c). This results in enhanced overlap of the hydration shells and structural rearrangements which inhibits translational dynamics. The calculated values for $D_{||}$ as a function of distance from the hydrophilic calcite surface are lower than those of water confined in hydrophobic pores ([2,53,54]. The strong reduction

of $D_{||}$ near hydrophilic surfaces is associated with the high water density and structuring in contrast to hydrophobic surfaces where the weak slow down has been related to formation short lived ice-like structures[2].

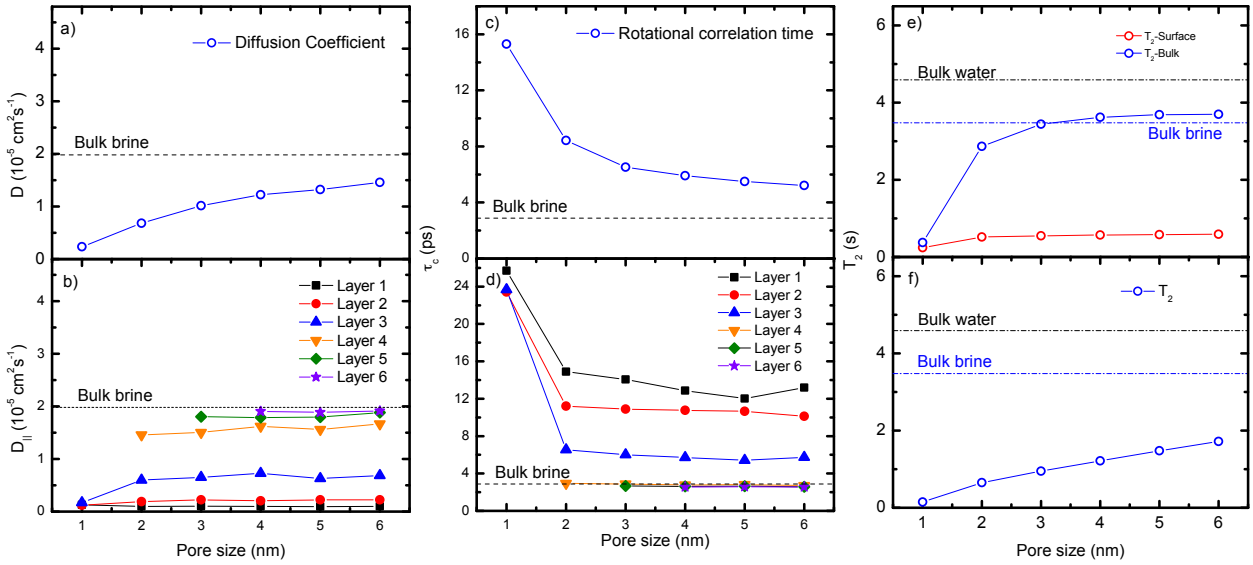

Figure 5: a) 3D self-diffusion coefficient of water molecules in the confined API brine solution as a function of pore size. b) Parallel 2D self-diffusion coefficient as a function of distance from the calcite surface and pore size. Error bars from the fitting of the MSD data are smaller than the symbol sizes. c) Rotational correlation time for all the water in API brine inside calcite slit pores. d) Rotational correlation time as a function of distance from the surface. Error bars from the exponential fitting are roughly the same size as the symbols. e) T_2 relaxation time of confined water in API brine on the surface and bulk-like region of calcite 1–6 nm pores. f) Total T_2 relaxation time as a function of pore size. The propagated errors are too small to be represented in this graph.

Reorientational dynamics

The longer the rotational correlation time τ_c, the slower is the molecular reorientation, thereby, revealing restrictions in the rotational degrees of freedom of hydrogen bonds[55]. According to Figure 5c, τ_c decreases with increasing pore size, with a slowdown factor of 5.3 for a 1 nm pore and 1.8 for a 6 nm pore, in comparison to bulk API brine. Previous studies[5,56,57] have associated this slowdown on reorientational dynamics of confined pure water to the slightly enhanced hydrogen bond strength caused by spatial confinement. In addition, the presence of ions in our system breaks the hydrogen bond network as evidenced by the degree distribution (Figure 3c). The immediate consequence of this is the reduction

of the number of accessible states for water reorientation, leading to reduced reorientations due to steric effect[58]. Furthermore, molecular dynamics studies on aqueous solutions[58,59] have shown that the electrostatic interactions of water oxygen with Na^+, Cl^- and Ca^{2+} ions is greater than the water-water hydrogen bond, which explains the further hindrance of the reorientational dynamics for water molecules in brine solution.

The local reorientational dynamics investigated from layer by layer analysis indicates that water molecules in layers 1 and 2 have the slowest reorientational dynamics as expected for hydrophilic surfaces. Despite the absence of ions in these layers, τ_c is slightly higher than for confined pure water[5]. This is an indication that the ions which appear in layer 3 slightly stabilize the water reorientation on the adsorption layer, highlighted here to be a direct effect of the local structuring of the water and ions (see Figures 1a–d) along the surface normal. The significance of the structure makers (Na^+ ions) and breakers (Cl^- ions) is evident from the τ_c values obtained in layers 3–6; high relative density of structure makers (breakers) results in longer (shorter) τ_c in comparison to bulk brine[58]. Although Ca^{2+} ions are structure makers, their small concentration has minor effect at the center of the pores. The uniformity of the values in layers 4–6 demonstrates that the surface has negligible effects on the rotational dynamics in this region of the pore.

For the system with 1 nm pore size, the τ_c values obtained for each layer indicates that the water is highly immobile as compared to larger pores (See Figure S9 for the behavior of $C_{HH}(t)$ in a 1 nm pore in comparison to 2 and 6 nm pores). The arrangement of water and ions within the 1 nm pore (Figure 1c), means that most of the water-water hydrogen bonds are exchanged for water-ion interactions or water-surface bonds. The resultant τ_c is long, an implication that for a high concentration of ions, the relative contribution of structure makers and breakers is indistinguishable and the collective effect is dominant for structure makers. These findings are in agreement with molecular dynamics simulations of water in concentrated solutions[58].

Transverse spin relaxation

As a very sensitive indicator of local mobility and the binding state of water in porous media, the transverse relaxation time (T_2) is an important parameter to characterize calcite–brine interactions. Spin relaxation can arise from translational as well as rotational dynamics[60], and thereby, any fluctuations can affect the measured value of T_2. We observed that calcite water interaction affect mainly the surface water (layers 1 and 2) resulting in T_2 value one order of magnitude lower than for bulk–like water (see Figure 5e). Except for the 1 nm pore which display high ionic concentration near surface layer, the T_2 value for the water molecules in the surface layer is similar to the value for pure water confined in calcite slit pores[5]. It can be inferred from this study that for pores of at least 2 nm, the physical and electrostatic barrier created by the water molecules on the calcite surface leads to similar T_2 on the surface for both confined pure water and brine solutions due the absence of ions in this region. This low T_2 value observed on the surface layer of water can be viewed as a measure of the attractive "wetting" character of the calcite surface by the fluid[61]. These findings are in qualitative agreement with experimental observations that surface interactions help in lowering the relaxation times[62,63].

In the bulk-like region (formed by layers ranging from 4 to 6), the relaxation of water molecules is highly pore size dependent. For the calcite pores studied here, the relaxation time reaches the bulk API brine T_2 relaxation time for pores with sizes ranging from 3 to 6 nm. Other than the confinement, an additional factor for the bulk-like region relaxation time is the ionic concentration since in general, Na^+ and Ca^{2+} ions decrease while Cl^- ions slightly increase the NMR relaxation time[64,65]. For the bulk API brine, the collective effects of these ions is to reduce the NMR T_2 relaxation time to 3.48 s in comparison to 4.59 s[5] for bulk water obtained from MD simulations. We show that for the larger pores (4 to 6 nm) where the surface has negligible effects in the bulk-like region, there is slight increase of the T_2 relaxation time which we attribute to the high density of Cl^-. This behavior correlates with the local rotational dynamics, which indicates that translational

dynamics have negligible effect on the T_2 relaxation in the bulk-like region. In contrast, the T_2 relaxation time in the bulk-like region is relatively shorter than the bulk API brine for the smaller pores. Specifically for the 1 nm pore, we establish a limit of the fast exchange model, which is valid for small pores as long as separate surface and bulk-like phases exist. The high concentration of ions in the 1 nm pore center leads to a spin relaxation in layer 3, which is comparable to the surface layers (layer 1 and layer 2) making it difficult to clearly separate the surface and bulk phases.

The total T_2 relaxation time of the confined API brine averaged over the surface and bulk-like regions according to Brownstein and Tarr model[33] is shown in Figure 5f. The trend of the NMR T_2 relaxation time studied in calcite pores reflects the general sensitivity of NMR measurements to pore-size distributions, where a lower T_2 is expected for small pores, whereas, large pores result in higher T_2 values. The experimental T_2 cutoff for carbonates is in the order of hundreds of ms[66], which is comparatively shorter than our calculated values. This is expected, since, in our theoretical model the dipolar interactions are only modulated by hindered molecular dynamics which is not the only relaxation mechanism in natural rocks[67]. In comparison to pure water confined in calcite, the presence of ions slightly lower the T_2 relaxation time[5]. The reasons for this change is two fold: on the one hand, spin relaxation arising from translational diffusion is attenuated as a consequence of the distortions on the hydrogen bond network (Figures 4a–c). On the other hand, the unbalanced concentration between structure makers and breakers observed mainly in bulk-like region in the brine solution slightly increase the rotational spin relaxation. Considering that the surface dominates the observed T_2 in porous media[60], the T_2 values measured in this kind of systems is expected to be dependent on the properties of the surface water. For small pores (as shown here for a 1 nm pore) and/or for systems with high ionic concentrations, the ions play a significant role on the obtained T_2 values.

Conclusion

We provided a fresh molecular look with significant insight toward the discussion about the effect of confinement interfaces and ions from electrolyte aqueous solutions on liquid water structure and dynamics. To properly address the system properties, we adopt an original approach by combining molecular dynamics simulations with hydrogen bond network analysis based on graph theory and NMR modeling. Our main contributions are on describing the structure of solvent and ions at calcite-solution interfaces and its physical indications and potential significance on the crystal growth and dissolution processes.

The particular ionic distribution observed inside the calcite slit pore is related with the spatially alternated electrostatic potential which arise from the strong ordering of water molecules in contact with the solid surface interface (Figures 2a–d). As a consequence, the Na^+ and Cl^- ions occupy respectively, the negative and positive accumulation regions observed in water 2D charge density profile, while Ca^{2+} ions are located mainly on the pore center due to their high hydration shell. In particular, the Na^+ and Cl^- electrolyte ions occupy the available sites near at the solid/brine interface resulting in a screening effect[68], thus reducing the probability of desolvating and attaching of foreign chemical species directly on the surface[69]. Such response can influence the crystal growth and can explain the results obtained experimentally on scale formation in hardwater pipes[70]. The authors related the growth rate with the surface wettabillity, and they argue that hydrophilicity decrease the calcium carbonate uptake because such particle must compete with pre-existing solid-solution interactions.

We observed the hydrogen bond structure (Figures 3a–c) and particle density (Figure 1a) of water belonging to the adsorption layer is negligibly affected by the API brine. None of the considered ions reach the calcite surface due to the 1) electrostatic potential barrier which arise from the ordering water molecules belonging to the surface layer, and 2) the physical barrier imposed by the surface ice-like structure characterized by high coordinated water molecules and slow T_2. These results revealed an additional mechanism displayed by

calcite surface able to inhibit the formation of pathways for the crystal growth, thus should be considered in the crystallization models. The hydrogen bond network is temperature sensitive[44], and therefore, the barrier imposed by surface water can be lowered by heating process. Temperature growth rate dependences are observed by several authors in both biogenic[71] and inorganic[72] crystallization, and according to our interpretation, such response can be related to this particular water structure.

Furthermore, the effect of ions on the branched aspect of water hydrogen bond network was properly characterized through the geodesic path analysis based on graph theory. We revealed that larger geodesic paths are displayed to connect two spatially separated water molecules to overcome or contour the network discontinuity imposed by the salty ions and the calcite surface (see Figures 4a–c). Large geodesic paths are extended across the pores and they connect surface water with high dynamics molecules at the pore center. Specially, systems with 2 and 1 nm pore size exhibit high percent of the geodesic paths connecting the two surface water regions (see Figure S6). Considering the effect on the potential energy (see Figure S7) due to the path folding, such water structure can explain the glue-like mechanical properties observed in confinement environment by several authors[46,47]. The overall slow-down in water diffusion noticed with NMR modeling (see Figures 5a–b) is attributed to this particular distortions on the hydrogen bond network. It can influence the crystal growth rate by particle attachment, since the hydrated particle may take longer time to reach to an attachment site at the calcite surface[73].

Such particular hydrogen bond network revealed in current work has dramatic consequences on water dynamics and they are intimately related. The translational and rotational dynamics are uncorrelated, and our results show that the faster rotation at the center of the pores is due to the high density of Cl^- ions in this region. On the contrary, the global nature of the translational motions lead to a universal low diffusion coefficient regardless of the nature of ions. Although the surface has the greatest effect on the relaxation time, the enhanced dipolar interactions due to a more folded hydrogen bond network further slows down

the calculated T_2 relaxation time of brine in confinement. Our findings obtained by NMR modeling complement the experimental measurements of aqueous solutions in nanoscopic media by providing useful measures of pertinent parameters.

Supporting Information Available

Detailed description of the system setup; complementary results about the geodesic analysis; additional information related to the water diffusion and the rotational correlation function. This material is available free of charge via the Internet at `http://pubs.acs.org/`.

Acknowledgement

The authors gratefully acknowledge the financial support from PETROBRAS and CNPq, CAPES and FAPESP funding agencies.

References

(1) Han, S.; Choi, M.; Kumar, P.; Stanley, H. E. Phase transitions in confined water nanofilms. *Nat. Phys.* **2010**, *6*, 685–689.

(2) Romero-Vargas Castrillon, S.; Giovambattista, N.; Aksay, I. A.; Debenedetti, P. G. Effect of surface polarity on the structure and dynamics of water in nanoscale confinement. *J. Phys. Chem. B* **2009**, *113*, 1438–1446.

(3) Branson, O.; Bonnin, E. A.; Perea, D. E.; Spero, H. J.; Zhu, Z.; Winters, M.; Hönisch, B.; Russell, A. D.; Fehrenbacher, J. S.; Gagnon, A. C. Nanometer-scale chemistry of a calcite biomineralization template: implications for skeletal composition and nucleation. *Proc. Natl. Acad. Sci.* **2016**, *113*, 12934–12939.

(4) De Yoreo, J. J.; Gilbert, P. U.; Sommerdijk, N. A.; Penn, R. L.; Whitelam, S.; Joester, D.; Zhang, H.; Rimer, J. D.; Navrotsky, A.; Banfield, J. F. Crystallization by particle attachment in synthetic, biogenic, and geologic environments. *Science* **2015**, *349*, aaa6760.

(5) Mutisya, S. M.; Kirch, A.; de Almeida, J. M.; Sanchez, V. M.; Miranda, C. R. Molecular dynamics simulations of water confined in calcite slit Pores: an NMR spin relaxation and hydrogen bond analysis. *J. Phys. Chem. C* **2017**, *121*, 6674–6684.

(6) Mancinelli, R. The effect of confinement on water structure. *J. Phys.: Condens. Matter* **2010**, *22*, 404213.

(7) Dore, J. Structural studies of water in confined geometry by neutron diffraction. *Chem. Phys.* **2000**, *258*, 327–347.

(8) Bellissent-Funel, M.-C.; Bradley, K.; Chen, S.; Lal, J.; Teixeira, J. Slow dynamics of water molecules in confined space. *Physica A* **1993**, *201*, 277–285.

(9) Mukhopadhyay, A.; Zhao, J.; Bae, S. C.; Granick, S. Contrasting friction and diffusion in molecularly thin confined films. *Phys. Rev. Lett.* **2002**, *89*, 136103.

(10) Sakuma, H.; Otsuki, K.; Kurihara, K. Viscosity and lubricity of aqueous NaCl solution confined between mica surfaces studied by shear resonance measurement. *Phys. Rev. Lett.* **2006**, *96*, 046104.

(11) Marcus, Y. Effect of ions on the structure of water. *Pure Appl. Chem.* **2010**, *82*, 1889–1899.

(12) Marcus, Y. Effect of ions on the structure of water: structure making and breaking. *Chem. Rev.* **2009**, *109*, 1346–1370.

(13) Paschek, D.; Ludwig, R. Specific ion effects on water structure and dynamics beyond the first hydration shell. *Angew. Chem., Int. Ed.* **2011**, *50*, 352–353.

(14) Holzmann, J.; Ludwig, R.; Geiger, A.; Paschek, D. Pressure and salt effects in simulated water: Two sides of the same coin? *Angew. Chem., Int. Ed.* **2007**, *46*, 8907–8911.

(15) Park, S.; Moilanen, D. E.; Fayer, M. D. Water dynamics the effects of ions and nanoconfinement. *J. Phys. Chem. B* **2008**, *112*, 5279–5290.

(16) Bakli, C.; Chakraborty, S. Effect of presence of salt on the dynamics of water in uncharged nanochannels. *J. Chem. Phys.* **2013**, *138*, 054504.

(17) Spagnoli, D.; Cooke, D. J.; Kerisit, S.; Parker, S. C. Molecular dynamics simulations of the interaction between the surfaces of polar solids and aqueous solutions. *J. Mater. Chem.* **2006**, *16*, 1997–2006.

(18) Argyris, D.; Cole, D. R.; Striolo, A. Ion-specific effects under confinement: the role of interfacial water. *ACS Nano* **2010**, *4*, 2035–2042.

(19) Khan, S. H.; Kramkowski, E. L.; Hoffmann, P. M. NaCl-dependent ordering and dynamic mechanical response in nanoconfined water. *Langmuir* **2016**, *32*, 10802–10807.

(20) Le Caër, S.; Lima, M.; Gosset, D.; Simeone, D.; Bergaya, F.; Pommeret, S.; Renault, J.-P.; Righini, R. Dynamics of water confined in clay minerals. *J. Phys. Chem. C* **2012**, *116*, 12916–12925.

(21) Ricci, M.; Spijker, P.; Stellacci, F.; Molinari, J.-F.; Voïtchovsky, K. Direct visualization of single ions in the Stern layer of calcite. *Langmuir* **2013**, *29*, 2207–2216.

(22) Plimpton, S. Fast parallel algorithms for short-range molecular dynamics. *J. Comput. Phys.* **1995**, *117*, 1–19.

(23) Nosé, S. A unified formulation of the constant temperature molecular dynamics methods. *J. Chem. Phys.* **1984**, *81*, 511–519.

(24) Melchionna, S.; Ciccotti, G.; Lee Holian, B. Hoover NPT dynamics for systems varying in shape and size. *Mol. Phys.* **1993**, *78*, 533–544.

(25) Beckers, J.; Lowe, C.; De Leeuw, S. An iterative PPPM method for simulating Coulombic systems on distributed memory parallel computers. *Mol. Simul.* **1998**, *20*, 369–383.

(26) Raiteri, P.; Gale, J. D.; Quigley, D.; Rodger, P. M. Derivation of an accurate force-field for simulating the growth of calcium carbonate from aqueous solution: A new model for the calcite- water interface. *J. Phys. Chem. C* **2010**, *114*, 5997–6010.

(27) Raiteri, P.; Gale, J. D. Water is the key to nonclassical nucleation of amorphous calcium carbonate. *J. Am. Chem. Soc.* **2010**, *132*, 17623–17634.

(28) Wu, Y.; Tepper, H. L.; Voth, G. A. Flexible simple point-charge water model with improved liquid-state properties. *J. Chem. Phys.* **2006**, *124*, 024503.

(29) Grossfield, A.; Ren, P.; Ponder, J. W. Ion solvation thermodynamics from simulation with a polarizable force field. *J. Am. Chem. Soc.* **2003**, *125*, 15671–15682.

(30) Allen, M. P.; Tildesley, D. J. *Computer simulation of liquids*; Oxford university press, 1989.

(31) Van der Maarel, J.; Lankhorst, D.; De Bleijser, J.; Leyte, J. Water dynamics in aqueous electrolyte solutions from proton, deuterium and oxygen-17 nuclear magnetic relaxation. *J. Phys. Chem.* **1986**, *90*, 1470–1478.

(32) Bloembergen, N.; Purcell, E. M.; Pound, R. V. Relaxation effects in nuclear magnetic resonance absorption. *Phys. Rev.* **1948**, *73*, 679.

(33) Brownstein, K. R.; Tarr, C. Importance of classical diffusion in NMR studies of water in biological cells. *Phys. Rev. A* **1979**, *19*, 2446.

(34) Cohen, M. H.; Mendelson, K. S. Nuclear magnetic relaxation and the internal geometry of sedimentary rocks. *J. Appl. Phys.* **1982**, *53*, 1127–1135.

(35) Markgraf, S. A.; Reeder, R. J. High-temperature structure refinements of calcite and magnesite. *Am. Mineral.* **1985**, *70*, 590–600.

(36) Skinner, A. J.; LaFemina, J. P.; Jansen, H. J. Structure and bonding of calcite; a theoretical study. *Am. Mineral.* **1994**, *79*, 205–214.

(37) Heberling, F.; Trainor, T. P.; Lützenkirchen, J.; Eng, P.; Denecke, M. A.; Bosbach, D. Structure and reactivity of the calcite–water interface. *J. Colloid Interface Sci.* **2011**, *354*, 843–857.

(38) MacInnis, I. N.; Brantley, S. L. The role of dislocations and surface morphology in calcite dissolution. *Geochim. Cosmochim. Acta* **1992**, *56*, 1113–1126.

(39) Martínez, L.; Andrade, R.; Birgin, E. G.; Martínez, J. M. PACKMOL: a package for building initial configurations for molecular dynamics simulations. *J. Comput. Chem.* **2009**, *30*, 2157–2164.

(40) Bourg, I. C.; Sposito, G. Molecular dynamics simulations of the electrical double layer on smectite surfaces contacting concentrated mixed electrolyte (NaCl–CaCl 2) solutions. *J. Colloid Interface Sci.* **2011**, *360*, 701–715.

(41) Kerisit, S.; Parker, S. C. Free energy of adsorption of water and metal ions on the {1014} calcite surface. *J. Am. Chem. Soc.* **2004**, *126*, 10152–10161.

(42) Marutschke, C.; Walters, D.; Cleveland, J.; Hermes, I.; Bechstein, R.; Kühnle, A. Three-dimensional hydration layer mapping on the (10.4) surface of calcite using amplitude modulation atomic force microscopy. *Nanotechnology* **2014**, *25*, 335703.

(43) Stipp, S. Toward a conceptual model of the calcite surface: hydration, hydrolysis, and surface potential. *Geochim. Cosmochim. Acta* **1999**, *63*, 3121–3131.

(44) Ozkanlar, A.; Clark, A. E. ChemNetworks: A complex network analysis tool for chemical systems. *J. Comput. Chem.* **2014**, *35*, 495–505.

(45) Ricci, M. A.; Bruni, F.; Giuliani, A. "Similarities" between confined and supercooled water. *Faraday Discuss.* **2009**, *141*, 347–358.

(46) Jinesh, K.; Frenken, J. Capillary condensation in atomic scale friction: how water acts like a glue. *Phys. Rev. Lett.* **2006**, *96*, 166103.

(47) Rossetto, H. L.; Bowen, J.; Kendall, K. Adhesion of alumina surfaces through confined water layers containing various molecules. *Langmuir* **2012**, *28*, 4648–4653.

(48) Fayer, M. D.; Levinger, N. E. Analysis of water in confined geometries and at interfaces. *Annu. Rev. Anal. Chem.* **2010**, *3*, 89–107.

(49) Fecko, C. J.; Eaves, J. D.; Loparo, J. J.; Tokmakoff, A.; Geissler, P. L. Ultrafast hydrogen-bond dynamics in the infrared spectroscopy of Water. *Science* **2003**, *301*, 1698–1702.

(50) Chiavazzo, E.; Fasano, M.; Asinari, P.; Decuzzi, P. Scaling behaviour for the water transport in nanoconfined geometries. *Nat. Commun.* **2014**, *5*.

(51) Jungwirth, P. Spiers memorial lecture ions at aqueous interfaces. *Faraday Discuss.* **2009**, *141*, 9–30.

(52) Kim, J. S.; Wu, Z.; Morrow, A. R.; Yethiraj, A.; Yethiraj, A. Self-diffusion and viscosity in electrolyte solutions. *J. Phys. Chem. B* **2012**, *116*, 12007–12013.

(53) Eslami, H.; Heydari, N. Hydrogen bonding in water nanoconfined between graphene surfaces: a molecular dynamics simulation study. *J. Nanopart. Res.* **2014**, *16*, 2154.

(54) Eslami, H.; Jaafari, B.; Mehdipour, N. Coarse grained molecular dynamics simulation of nanoconfined water. *ChemPhysChem* **2013**, *14*, 1063–1070.

(55) Bakker, H.; Woutersen, S.; Nienhuys, H.-K. Reorientational motion and hydrogen-bond stretching dynamics in liquid water. *Chem. Phys.* **2000**, *258*, 233–245.

(56) Fogarty, A. C.; Coudert, F.-X.; Boutin, A.; Laage, D. Reorientational dynamics of water confined in zeolites. *ChemPhysChem* **2014**, *15*, 521–529.

(57) Raviv, U.; Laurat, P.; Klein, J. Fluidity of water confined to subnanometer films. *Nature* **2001**, *413*, 51–54.

(58) Stirnemann, G.; Wernersson, E.; Jungwirth, P.; Laage, D. Mechanisms of acceleration and retardation of water dynamics by ions. *J. Am. Chem. Soc.* **2013**, *135*, 11824–11831.

(59) Fulton, J. L.; Heald, S. M.; Badyal, Y. S.; Simonson, J. Understanding the effects of concentration on the solvation structure of Ca2+ in aqueous solution. I: The perspective on local structure from EXAFS and XANES. *J. Phys. Chem. A* **2003**, *107*, 4688–4696.

(60) Kimmich, R. *Principles of soft-matter dynamics: basic theories, non-invasive methods, Mesoscopic Aspects*; Springer Science & Business Media, 2012.

(61) Senturia, S. D.; Robinson, J. Nuclear spin-lattice relaxation of liquids confined in porous solids. *Soc. Pet. Eng. J.* **1970**, *10*, 237–244.

(62) McDonald, P.; Korb, J.-P.; Mitchell, J.; Monteilhet, L. Surface relaxation and chemical exchange in hydrating cement pastes: a two-dimensional NMR relaxation study. *Phys. Rev. E* **2005**, *72*, 011409.

(63) Monteilhet, L.; Korb, J.-P.; Mitchell, J.; McDonald, P. Observation of exchange of micropore water in cement pastes by two-dimensional T2–T2 nuclear magnetic resonance relaxometry. *Phys. Rev. E* **2006**, *74*, 061404.

(64) Iwaya-Inoue, M.; Yoshimura, K.; Yamasaki, H.; Kaku, S. Characteristic changes in relaxation times of water protons in Vigna radiata seedlings exposed to temperature stress. *Plant Cell Physiol.* **1993**, *34*, 705–711.

(65) Engel, G.; Hertz, H. On the negative hydration. A nuclear magnetic relaxation study. *Berich Bunsen Gesell* **1968**, *72*, 808–834.

(66) Westphal, H.; Surholt, I.; Kiesl, C.; Thern, H. F.; Kruspe, T. NMR measurements in

carbonate rocks: Problems and an approach to a solution. *Pure Appl. Geophys.* **2005**, *162*, 549–570.

(67) Kleinberg, R.; Kenyon, W.; Mitra, P. Mechanism of NMR relaxation of fluids in rock. *J. Magn. Reson., Ser. A* **1994**, *108*, 206–214.

(68) Chen, H.; Panagiotopoulos, A. Z.; Giannelis, E. P. Atomistic molecular dynamics simulations of carbohydrate–calcite interactions in concentrated brine. *Langmuir* **2015**, *31*, 2407–2413.

(69) Stephenson, A.; Hunter, J.; Han, N.; DeYoreo, J.; Dove, P. Effect of ionic strength on the Mg content of calcite: Toward a physical basis for minor element uptake during step growth. *Geochim. Cosmochim. Acta* **2011**, *75*, 4340–4350.

(70) Chevalier, N. R. Do surface wetting properties affect calcium carbonate heterogeneous nucleation and adhesion? *J. Phys. Chem. C* **2014**, *118*, 17600–17607.

(71) Eggins, S. M.; Sadekov, A.; De Deckker, P. Modulation and daily banding of Mg/Ca in Orbulina universa tests by symbiont photosynthesis and respiration: a complication for seawater thermometry? *Earth Planet. Sci. Lett.* **2004**, *225*, 411–419.

(72) Lea, D. W.; Mashiotta, T. A.; Spero, H. J. Controls on magnesium and strontium uptake in planktonic foraminifera determined by live culturing. *Geochim. Cosmochim. Acta* **1999**, *63*, 2369–2379.

(73) Wasylenki, L. E.; Dove, P. M.; De Yoreo, J. J. Effects of temperature and transport conditions on calcite growth in the presence of Mg2+: implications for paleothermometry. *Geochim. Cosmochim. Acta* **2005**, *69*, 4227–4236.

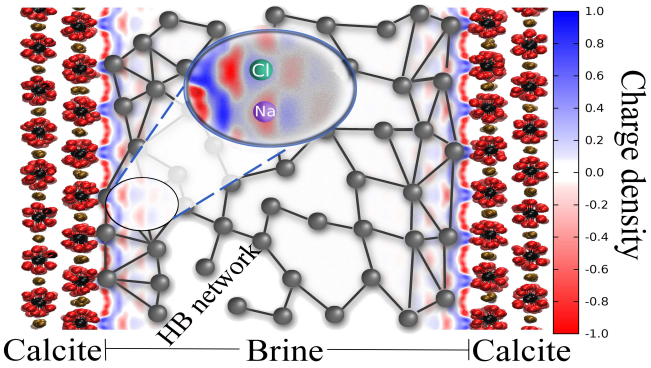
Cl
Na
HB network
Calcite
Brine
Calcite
Charge density
1.0
0.8
0.6
0.4
0.2
0.0
-0.2
-0.4
-0.6
-0.8
-1.0

TOC graphic